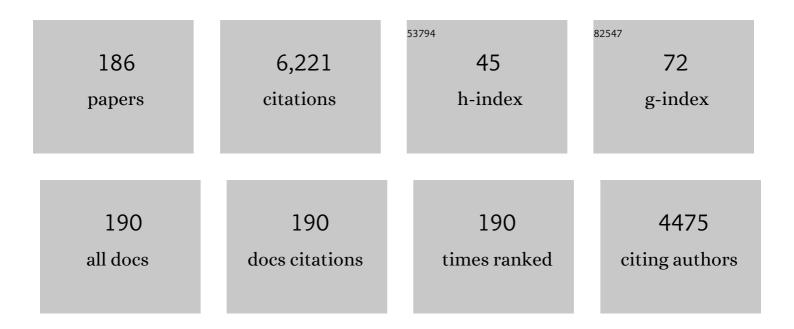
List of Publications by Year in descending order

Source: https://exaly.com/author-pdf/4704767/publications.pdf Version: 2024-02-01



FDANK FONST

#	Article	IF	CITATIONS
1	Quantitative assessment of nanoparticle size distributions from HRTEM images. International Journal of Materials Research, 2022, 97, 928-933.	0.3	0
2	Understanding the efficacy of concentrated interstitial carbon in enhancing the pitting corrosion resistance of stainless steel. Acta Materialia, 2021, 221, 117433.	7.9	24
3	Rapid Alloy Surface Engineering through Closed-Vessel Reagent Pyrolysis. Metals, 2021, 11, 1764.	2.3	2
4	High-temperature phase transformations in AISI 316 stainless steel infused with concentrated interstitial carbon. Journal of Alloys and Compounds, 2020, 819, 153000.	5.5	7
5	Low-Temperature Nitridation of 2205 Duplex Stainless Steel. Metallurgical and Materials Transactions A: Physical Metallurgy and Materials Science, 2020, 51, 608-617.	2.2	11
6	Stress–Corrosion Cracking of AISI 316L Stainless Steel in Seawater Environments: Effect of Surface Machining. Metals, 2020, 10, 1324.	2.3	12
7	The passivity of low-temperature carburized austenitic stainless steel AISI-316L in a simulated boiling-water-reactor environment. Journal of Nuclear Materials, 2020, 537, 152197.	2.7	7
8	Surface engineering of IN-718 by low-temperature carburisation: properties and thermal stability. Surface Engineering, 2019, 35, 281-293.	2.2	4
9	Co–Cr–Mo alloys: Improved wear resistance through low-temperature gas-phase nitro-carburization. Surface and Coatings Technology, 2019, 378, 124943.	4.8	17
10	Effect of tungsten alloying on magnetic properties of amorphous Ni-P. Journal of Alloys and Compounds, 2019, 786, 742-749.	5.5	5
11	Electronic impact of concentrated interstitial carbon on physical properties of AISI-316 austenitic stainless steel. Acta Materialia, 2019, 173, 96-105.	7.9	12
12	Ultrahigh-strength AISI-316 austenitic stainless steel foils through concentrated interstitial carbon. Acta Materialia, 2019, 167, 231-240.	7.9	19
13	Stress–Corrosion Cracking of Surface-Engineered Alloys in a Simulated Boiling-Water Reactor Environment. Corrosion, 2018, 74, 635-653.	1.1	5
14	Low-Temperature Carburization of AL-6XN Enabled by Provisional Passivation. Metals, 2018, 8, 997.	2.3	9
15	Effect of lubricant additives on the tribological behavior of aluminum alloy against steel. International Journal of Materials Research, 2018, 109, 789-802.	0.3	6
16	Thermal stability of low-temperature-carburized austenitic stainless steel. Acta Materialia, 2017, 128, 235-240.	7.9	28
17	"Colossal―interstitial supersaturation in delta ferrite in stainless steels: (II) low-temperature nitridation of the 17-7ÂPH alloy. Acta Materialia, 2017, 124, 237-246.	7.9	9
18	Background of SAM atom-fraction profiles. Materials Characterization, 2017, 125, 142-151.	4.4	4

#	Article	IF	CITATIONS
19	The Formation of Martensitic Austenite During Nitridation of Martensitic and Duplex Stainless Steels. Metallurgical and Materials Transactions A: Physical Metallurgy and Materials Science, 2017, 48, 8-13.	2.2	7
20	Effect of tungsten alloying on short-to-medium-range-order evolution and crystallization behavior of near-eutectic amorphous Ni–P. Acta Materialia, 2017, 122, 400-411.	7.9	13
21	"Colossal―Interstitial Supersaturation in Delta Ferrite in 17-7 PH Stainless Steels After Low-temperature Nitridation. Microscopy and Microanalysis, 2016, 22, 2020-2023.	0.4	0
22	Electroless Deposition of Copper-Manganese for Applications in Semiconductor Interconnect Metallization. Journal of the Electrochemical Society, 2016, 163, D374-D378.	2.9	8
23	Corrosion-Resistant Alloys: Case Hardening. , 2016, , 947-962.		0
24	Crystallization micro-mechanism of near-eutectic amorphous Ni–P. Acta Materialia, 2016, 104, 274-282.	7.9	27
25	Increasing the coefficient of sliding friction of NiCr at low loads by interstitial surface hardening. Wear, 2016, 346-347, 1-5.	3.1	3
26	Crystallization of Ni–P Fabricated by Electroless Deposition: Microscopic Mechanism. Materials Research Society Symposia Proceedings, 2015, 1757, 20.	0.1	2
27	"Colossal―interstitial supersaturation in delta ferrite in stainless steels—I. Low-temperature carburization. Acta Materialia, 2015, 86, 193-207.	7.9	18
28	NiAl precipitation in delta ferrite grains of 17-7 precipitation-hardening stainless steel during low-temperature interstitial hardening. Scripta Materialia, 2015, 108, 136-140.	5.2	6
29	Properties of the Passive Film Formed on Interstitially Hardened AISI 316L Stainless Steel. Electrochimica Acta, 2015, 176, 410-419.	5.2	29
30	Diffusion profiles after nitrocarburizing austenitic stainless steel. Surface and Coatings Technology, 2015, 279, 180-185.	4.8	21
31	The Effect of Surface Finish on Low-Temperature Acetylene-Based Carburization of 316L Austenitic Stainless Steel. Metallurgical and Materials Transactions B: Process Metallurgy and Materials Processing Science, 2014, 45, 2338-2345.	2.1	7
32	Orientation dependence of nitrogen supersaturation in austenitic stainless steel during low-temperature gas-phase nitriding. Acta Materialia, 2014, 79, 339-350.	7.9	60
33	Cellular Precipitation at a 17-7 PH Stainless Steel Interphase Interface During Low-Temperature Nitridation. Metallurgical and Materials Transactions A: Physical Metallurgy and Materials Science, 2014, 45, 3578-3585.	2.2	13
34	Concentration-Dependent Carbon Diffusivity in Austenite. Metallurgical and Materials Transactions A: Physical Metallurgy and Materials Science, 2014, 45, 3790-3799.	2.2	10
35	Numerical Simulations of Carbon and Nitrogen Composition-Depth Profiles in Nitrocarburized Austenitic Stainless Steels. Metallurgical and Materials Transactions A: Physical Metallurgy and Materials Science, 2014, 45, 4268-4279.	2.2	29
36	Colossal Carbon Supersaturation of Delta Ferrite in 17-7 PH Stainless Steel. Microscopy and Microanalysis, 2014, 20, 2102-2103.	0.4	1

#	Article	IF	CITATIONS
37	Low-Temperature Carburization of Austenitic Stainless Steels. , 2014, , 451-460.		18
38	Highly Stable Pt–Au@Ru/C Catalyst Nanoparticles for Methanol Electro-oxidation. Journal of Physical Chemistry C, 2013, 117, 1457-1467.	3.1	36
39	Fatigue crack growth in interstitially hardened AISI 316L stainless steel. International Journal of Fatigue, 2013, 47, 100-105.	5.7	14
40	Auger Electron Spectroscopy of Carbon Diffusion Profiles in Low Temperature Carburized Stainless Steels. Microscopy and Microanalysis, 2013, 19, 1106-1107.	0.4	1
41	Interstitial hardening of duplex 2205 stainless steel by low temperature carburisation: enhanced mechanical and electrochemical performance. Surface Engineering, 2012, 28, 213-219.	2.2	21
42	The Platinumâ^•Titanium-Nitride Interface: X-Ray Photoelectron Spectroscopy Studies. Electrochemical and Solid-State Letters, 2012, 15, B79.	2.2	0
43	Sustained-load crack growth of hydrogen-charged surface-hardened 316L stainless steel. Materials Science & Engineering A: Structural Materials: Properties, Microstructure and Processing, 2012, 556, 43-50.	5.6	7
44	Volatility Diagrams for the Cr-O and Cr-Cl Systems: Application to Removal of Cr2O3-Rich Passive Films on Stainless Steel. Metallurgical and Materials Transactions B: Process Metallurgy and Materials Processing Science, 2012, 43, 1187-1201.	2.1	13
45	Enhanced corrosion resistance of interstitially hardened stainless steel: Implications of a critical passive layer thickness for breakdown. Acta Materialia, 2012, 60, 716-725.	7.9	65
46	Ferromagnetism in interstitially hardened austenitic stainless steel induced by low-temperature gas-phase nitriding. Scripta Materialia, 2011, 65, 1089-1092.	5.2	16
47	The carbide M7C3 in low-temperature-carburized austenitic stainless steel. Acta Materialia, 2011, 59, 2268-2276.	7.9	43
48	The Platinum/Titanium Nitride Interface: X-ray Photoelectron Spectroscopy Studies. ECS Transactions, 2011, 41, 865-874.	0.5	0
49	Microcharacterization of Tribo Layers on Al–Steel. Microscopy and Microanalysis, 2010, 16, 1560-1561.	0.4	Ο
50	Low-Temperature Carburization of the Ni-base Superalloy IN718: Improvements in Surface Hardness and Crevice Corrosion Resistance. Metallurgical and Materials Transactions A: Physical Metallurgy and Materials Science, 2010, 41, 2022-2032.	2.2	20
51	Synthesis, characterization of a CoSe2 catalyst for the oxygen reduction reaction. Applied Catalysis A: General, 2010, 386, 157-165.	4.3	50
52	Expansion of interatomic distances in platinum catalyst nanoparticles. Acta Materialia, 2010, 58, 836-845.	7.9	26
53	Carburization-Enhanced Passivity of PH13-8 Mo: A Precipitation-Hardened Martensitic Stainless Steel. Electrochemical and Solid-State Letters, 2010, 13, C37.	2.2	28
54	Wear maps for low temperature carburised 316L austenitic stainless steel sliding against alumina. Surface Engineering, 2010, 26, 284-292.	2.2	36

#	Article	IF	CITATIONS
55	Carbonâ€5upported, Seleniumâ€Modified Ruthenium–Molybdenum Catalysts for Oxygen Reduction in Acidic Media. ChemSusChem, 2009, 2, 658-664.	6.8	27
56	Poisson Effects on X-Ray Diffraction Patterns in Low-Temperature-Carburized Austenitic Stainless Steel. Metallurgical and Materials Transactions A: Physical Metallurgy and Materials Science, 2009, 40, 1799-1804.	2.2	39
57	Paraequilibrium Carburization of Duplex and Ferritic Stainless Steels. Metallurgical and Materials Transactions A: Physical Metallurgy and Materials Science, 2009, 40, 1781-1790.	2.2	21
58	Enhanced Carbon Diffusion in Austenitic Stainless Steel Carburized at Low Temperature. Metallurgical and Materials Transactions A: Physical Metallurgy and Materials Science, 2009, 40, 1768-1780.	2.2	47
59	Enhanced Corrosion Resistance of Stainless Steel Carburized at Low Temperature. Metallurgical and Materials Transactions A: Physical Metallurgy and Materials Science, 2009, 40, 1805-1810.	2.2	57
60	Fundamental Investigation of Oxygen Reduction Reaction on Rhodium Sulfide-Based Chalcogenides. Journal of Physical Chemistry C, 2009, 113, 6955-6968.	3.1	46
61	Formation of nickel nanoparticles in nickel – ceramic anodes during operation of solid-oxide fuel cells. International Journal of Materials Research, 2008, 99, 548-552.	0.3	9
62	Localized Corrosion Resistance of LTCSS-Carburized Materials to Seawater Immersion. ECS Transactions, 2007, 3, 613-621.	0.5	5
63	Local Electrode Atom Probe (LEAPTM) Tomographic Microanalysis of Low Temperature Gas Carburized Austenitic Stainless Steel. Microscopy and Microanalysis, 2007, 13, .	0.4	1
64	Carburization-Induced Passivity of 316 L Austenitic Stainless Steel. Electrochemical and Solid-State Letters, 2007, 10, C76.	2.2	59
65	Carbide precipitation in austenitic stainless steel carburized at low temperature. Acta Materialia, 2007, 55, 1895-1906.	7.9	97
66	Shear strength and sliding at a metal–ceramic (aluminum–spinel) interface at ambient and elevated temperatures. Acta Materialia, 2007, 55, 3049-3057.	7.9	19
67	Enhanced fatigue resistance in 316L austenitic stainless steel due to low-temperature paraequilibrium carburization. Acta Materialia, 2007, 55, 5572-5580.	7.9	75
68	Interstitial defects in 316L austenitic stainless steel containing "colossal―carbon concentrations: An internal friction study. Scripta Materialia, 2007, 56, 1067-1070.	5.2	36
69	Carbon supersaturation due to paraequilibrium carburization: Stainless steels with greatly improved mechanical properties. Acta Materialia, 2006, 54, 1597-1606.	7.9	161
70	Diffusion reactions at Al–MgAl2O4 interfaces—and the effect of applied electric fields. Journal of Materials Science, 2006, 41, 7785-7797.	3.7	13
71	Carbon paraequilibrium in austenitic stainless steel. Metallurgical and Materials Transactions A: Physical Metallurgy and Materials Science, 2006, 37, 1819-1824.	2.2	74
72	Quantitative assessment of nanoparticle size distributions from HRTEM images. International Journal of Materials Research, 2006, 97, 928-933.	0.3	11

#	Article	IF	CITATIONS
73	Gas-phase surface alloying under "kinetic control― A novel approach to improving the surface properties of titanium alloys. International Journal of Materials Research, 2006, 97, 597-606.	0.3	3
74	Liquid-phase deposition of single-phase alpha-copper-indium-diselenide. Materials Science and Engineering B: Solid-State Materials for Advanced Technology, 2005, 116, 311-319.	3.5	7
75	Epitaxial Growth of Cuprous Oxide Electrodeposited onto Semiconductor and Metal Substrates. Journal of the American Ceramic Society, 2005, 88, 253-270.	3.8	63
76	Surface hardening of Ti alloys by gas-phase nitridation: Kinetic control of the nitrogen surface activity. Metallurgical and Materials Transactions A: Physical Metallurgy and Materials Science, 2005, 36, 2429-2434.	2.2	25
77	Epitaxial Electrodeposition of High-Aspect-Ratio Cu2O(110) Nanostructures on InP(111). Chemistry of Materials, 2005, 17, 725-729.	6.7	74
78	Growth of ultra-thin and highly relaxed SiGe layers under in-situ introduction of point defects. EPJ Applied Physics, 2004, 27, 341-344.	0.7	5
79	In situ nanoscale observation and control of electron-beam-induced cluster formation. Journal of Vacuum Science & Technology an Official Journal of the American Vacuum Society B, Microelectronics Processing and Phenomena, 2004, 22, 1797.	1.6	5
80	Carbides in low-temperature-carburized stainless steels. Acta Materialia, 2004, 52, 1469-1477.	7.9	65
81	TEM Studies of Cu2O-Si and Cu2O-InP Interfaces Made by Epitaxial Electrodeposition. Microscopy and Microanalysis, 2004, 10, 292-293.	0.4	0
82	Preferred Intercrystalline Orientation Relationships and the Near Coincidence of Reciprocal Lattice Points. Microscopy and Microanalysis, 2004, 10, 264-265.	0.4	0
83	Colossal carbon supersaturation in austenitic stainless steels carburized at low temperature. Acta Materialia, 2003, 51, 4171-4181.	7.9	179
84	Epitaxial electrodeposition of Cu2O films onto InP(001). Applied Physics Letters, 2003, 83, 1944-1946.	3.3	49
85	Shape Control in Epitaxial Electrodeposition:  Cu2O Nanocubes on InP(001). Chemistry of Materials, 2003, 15, 4882-4885.	6.7	115
86	Microstructure of Cu2O/Si Interfaces, Made by Epitaxial Electrodeposition. International Journal of Materials Research, 2003, 94, 259-265.	0.8	3
87	Composition of self-assembled Ge/Si islands in single and multiple layers. Applied Physics Letters, 2002, 81, 2614-2616.	3.3	76
88	Assessing the mechanical strength of interfacial atomic bonds by quantitative high-resolution transmission electron microscopy. Philosophical Magazine A: Physics of Condensed Matter, Structure, Defects and Mechanical Properties, 2002, 82, 2677-2693.	0.6	3
89	Epitaxial Electrodeposition of a Crystalline Metal Oxide onto Single-Crystalline Silicon. Journal of Physical Chemistry B, 2002, 106, 12369-12372.	2.6	52
90	Self-Assembled Nanowire Networks by Deposition of Copper onto Layered-Crystal Surfaces. Advanced Materials, 2002, 14, 1056.	21.0	36

#	Article	lF	CITATIONS
91	Laterally aligned Ge/Si islands: a new concept for faster field-effect transistors. Materials Science and Engineering B: Solid-State Materials for Advanced Technology, 2002, 89, 101-105.	3.5	25
92	Diffusion of oxygen in CdSe-photosensor arrays. Materials Science and Engineering B: Solid-State Materials for Advanced Technology, 2002, 94, 123-130.	3.5	2
93	Fabrication of Cu-induced networks of linear nanostructures on different length scales. Acta Materialia, 2002, 50, 4925-4933.	7.9	6
94	Epitaxy of Ge on sapphire. Materials Science & Engineering A: Structural Materials: Properties, Microstructure and Processing, 2002, 323, 9-16.	5.6	10
95	Atomistic and electronic structure of Al/MgAl2O4and Ag/MgAl2O4interfaces. Philosophical Magazine A: Physics of Condensed Matter, Structure, Defects and Mechanical Properties, 2001, 81, 927-955.	0.6	49
96	Quantitative Analysis of Interface Structure by HRTEM. Microscopy and Microanalysis, 2001, 7, 240-241.	0.4	0
97	Self-Ordering of Ge Islands on Si Substrates Mediated by Local Strain Fields. Physica Status Solidi (B): Basic Research, 2001, 224, 531-535.	1.5	8
98	Fully relaxed Si0.7Ge0.3 buffers grown on patterned silicon substrates for hetero-CMOS transistors. Journal of Materials Science: Materials in Electronics, 2001, 12, 235-240.	2.2	3
99	Origin of diffuse electron scattering in yttria-cubicstabilized zirconia single crystals with 24–32 mol% yttria. Philosophical Magazine A: Physics of Condensed Matter, Structure, Defects and Mechanical Properties, 2001, 81, 1675-1689.	0.6	18
100	Preferred Grain Orientation Relationships in Sintered Perovskite Ceramics. Journal of the American Ceramic Society, 2001, 84, 1885-1890.	3.8	33
101	Atomistic and electronic structure of Al/MgAl2O4 and Ag/MgAl2O4 interfaces. Philosophical Magazine A: Physics of Condensed Matter, Structure, Defects and Mechanical Properties, 2001, 81, 927-955.	0.6	1
102	Carbon Nanotubes as Nanoreactors for Boriding Iron Nanowires. Advanced Materials, 2000, 12, 1356-1359.	21.0	37
103	Growth and microstructure of Ga2O3 nanorods. Solid State Communications, 2000, 115, 527-529.	1.9	70
104	Relaxed SiGe buffers with thicknesses below 0.1 \hat{l} ¼m. Thin Solid Films, 2000, 369, 152-156.	1.8	57
105	Step bunching and correlated SiGe nanostructures on Si(113). Thin Solid Films, 2000, 369, 39-42.	1.8	8
106	Preparation and optical properties of Ge and C-induced Ge quantum dots on Si. Thin Solid Films, 2000, 373, 164-169.	1.8	26
107	Relaxed SiCe buffer layer growth with point defect injection. Materials Science and Engineering B: Solid-State Materials for Advanced Technology, 2000, 71, 14-19.	3.5	17
108	Reduced critical thickness and photoluminescence line splitting in multiple layers of self-assembled Ge/Si islands. Materials Science and Engineering B: Solid-State Materials for Advanced Technology, 2000, 74, 248-252.	3.5	9

#	Article	IF	CITATIONS
109	Self-organized periodic arrays of SiGe wires and Ge islands on vicinal Si substrates. Physica E: Low-Dimensional Systems and Nanostructures, 2000, 7, 881-886.	2.7	22
110	Vertical correlation of SiGe islands in SiGe/Si superlattices: X-ray diffraction versus transmission electron microscopy. Applied Physics Letters, 2000, 77, 3953-3955.	3.3	22
111	Synthesis of GaN–carbon composite nanotubes and GaN nanorods by arc discharge in nitrogen atmosphere. Applied Physics Letters, 2000, 76, 652-654.	3.3	151
112	Effect of overgrowth temperature on the photoluminescence of Ge/Si islands. Applied Physics Letters, 2000, 77, 2509-2511.	3.3	72
113	Aligned CN[sub x] nanotubes by pyrolysis of ferrocene/C[sub 60] under NH[sub 3] atmosphere. Applied Physics Letters, 2000, 77, 1807.	3.3	112
114	Resonant tunneling diodes made up of stacked self-assembled Ge/Si islands. Applied Physics Letters, 2000, 77, 4341-4343.	3.3	44
115	Structure And Composition Of Grain Boundaries In SrTiO3. Microscopy and Microanalysis, 1999, 5, 94-95.	0.4	0
116	Interaction between Point Defects and Dislocations in SiGe. Solid State Phenomena, 1999, 69-70, 179-184.	0.3	6
117	Correlated SiGe wires shaped by regular step bunches on miscut Si(113) substrates. Physical Review B, 1999, 60, 10935-10940.	3.2	21
118	Structural investigation of Si/SiGe superlattices on vicinal (113) oriented Si. Thin Solid Films, 1999, 357, 71-75.	1.8	4
119	Structure and Composition of Grain Boundaries in Ceramics. Journal of the European Ceramic Society, 1999, 19, 665-673.	5.7	71
120	High-precision assessment of interface lattice offset by quantitative HRTEM. Journal of Microscopy, 1999, 194, 142-151.	1.8	26
121	Synthesizing boron nitride nanotubes filled with SiC nanowires by using carbon nanotubes as templates. Applied Physics Letters, 1999, 75, 1875-1877.	3.3	85
122	Formation of (BN)xCyand BN Nanotubes Filled with Boron Carbide Nanowires. Chemistry of Materials, 1999, 11, 3620-3623.	6.7	54
123	Micromechanisms of fracture in NiAl studied by in situ straining experiments in an HVEM. Intermetallics, 1999, 7, 479-489.	3.9	10
124	Self-Assembling Si/SiGe Nanostructures for Light Emitters. Solid State Phenomena, 1999, 69-70, 13-22.	0.3	7
125	Modified Stranski–Krastanov growth in stacked layers of self-assembled islands. Applied Physics Letters, 1999, 74, 1272-1274.	3.3	162
126	Germanium "quantum dots―embedded in silicon: Quantitative study of self-alignment and coarsening. Applied Physics Letters, 1999, 74, 269-271.	3.3	109

#	Article	IF	CITATIONS
127	Phase segregation, Cu migration and junction formation in Cu(In,ÂGa)Se2. EPJ Applied Physics, 1999, 6, 131-139.	0.7	121
128	Preparation and Optical Properties of Ge and C-Induced Ge Quantum Dots on Si. Materials Research Society Symposia Proceedings, 1999, 570, 187.	0.1	0
129	Preparation and Optical Properties of Ge and C-Induced Ge Quantum Dots on Si. Materials Research Society Symposia Proceedings, 1999, 571, 355.	0.1	0
130	Atomistic Structure of Σ = 3, (111) Grain Boundaries in Strontium Titanate. Physica Status Solidi A, 1998, 166, 57-71.	1.7	45
131	Influence of pre-grown carbon on the formation of germanium dots. Thin Solid Films, 1998, 321, 70-75.	1.8	25
132	Characterization of self-assembled Ge islands on Si(100) by atomic force microscopy and transmission electron microscopy. Thin Solid Films, 1998, 321, 86-91.	1.8	29
133	C-induced Ge dots: a versatile tool to fabricate ultra-small Ge nanostructures. Thin Solid Films, 1998, 336, 248-251.	1.8	22
134	Lateral ordering of self-assembled Ge islands. Thin Solid Films, 1998, 336, 252-255.	1.8	5
135	Atomistic structure of misfit dislocations in SrZrO3/SrTiO3 interfaces. Acta Materialia, 1998, 47, 183-198.	7.9	40
136	Reliability of atom column positions in a ternary system determined by quantitative highâ€resolution transmission electron microscopy. Journal of Microscopy, 1998, 190, 144-158.	1.8	24
137	Abâ€initioHRTEM simulations of ionic crystals: a case study of sapphire. Journal of Microscopy, 1998, 190, 89-98.	1.8	17
138	On Epitaxy and Orientation Relationships in Bicrystals. Solid State Phenomena, 1998, 59-60, 51-62.	0.3	12
139	Carbon-induced germanium dots: Kinetically-limited islanding process prevents coherent vertical alignment. Applied Physics Letters, 1998, 73, 659-661.	3.3	32
140	Theoretical and experimental investigations of structures and energies of Σ = 3, [112] tilt grain boundaries in copper. Philosophical Magazine A: Physics of Condensed Matter, Structure, Defects and Mechanical Properties, 1998, 77, 1161-1184.	0.6	52
141	Formation of carbon-induced germanium dots. Applied Physics Letters, 1997, 71, 2340-2342.	3.3	176
142	Microstructure and Optoelectronic Properties of CdSe-Thin Films. Materials Research Society Symposia Proceedings, 1997, 472, 131.	0.1	1
143	Present developments in high-resolution transmission electron microscopy. Current Opinion in Solid State and Materials Science, 1997, 2, 469-476.	11.5	15
144	Interface dislocations forming during epitaxial growth of GeSi on (111) Si substrates at high temperatures. Materials Science & Engineering A: Structural Materials: Properties, Microstructure and Processing, 1997, 233, 126-138.	5.6	10

#	Article	IF	CITATIONS
145	Effect of Shear Stress on the Atomistic Structure of a Grain Boundary in Strontium Titanate. Journal of the American Ceramic Society, 1997, 80, 1639-1644.	3.8	31
146	Quantitative High-Resolution Electron Microscopy of Interfaces. Materials Science Forum, 1996, 207-209, 23-34.	0.3	5
147	Analysis of Interface Structures by Quantitative High-Resolution Transmission Electron Microscopy. Materials Research Society Symposia Proceedings, 1996, 466, 95.	0.1	3
148	Quantification of irradiation damage generated during HRTEM with 1250 keV electrons. Ultramicroscopy, 1996, 63, 49-55.	1.9	12
149	Prediction of the BCC Structure in a Cu â~3-84° <211> Tilt Grain Boundary and Its Confirmation by HRTEM. Materials Science Forum, 1996, 207-209, 337-340.	0.3	1
150	Quantitative HRTEM of the â´3 (111) Grain Boundary in NiAl. Materials Science Forum, 1996, 207-209, 309-312.	0.3	3
151	The atomistic structure of a $\hat{l} \epsilon$ = 3, (111) grain boundary in NiAl, studied by quantitative high-resolution transmission electron microscopy. Philosophical Magazine A: Physics of Condensed Matter, Structure, Defects and Mechanical Properties, 1996, 74, 641-664.	0.6	28
152	Analysis of Grain-Boundary Structures by Quantitative Hrtem. Proceedings Annual Meeting Electron Microscopy Society of America, 1996, 54, 326-327.	0.0	0
153	Twin boundaries with 9R zone in Cu and Ag studied by quantitative HRTEM. Journal of Materials Science, 1995, 2, 201.	1.2	7
154	Dislocations in PbTiO3 Thin Films. Physica Status Solidi A, 1995, 147, 135-154.	1.7	66
155	Metal-oxide interfaces. Materials Science and Engineering Reports, 1995, 14, 97-156.	31.8	194
156	Domain configurations in ferroelectric PbTiO3 thin films: The influence of substrate and film thickness. Solid State Ionics, 1995, 75, 43-48.	2.7	36
157	Prediction and Observation of the bcc Structure in Pure Copper at aΣ3 Grain Boundary. Physical Review Letters, 1995, 75, 2160-2163.	7.8	56
158	The influence of Pt and SrTiO ₃ interlayers on the microstructure of PbTiO ₃ thin films deposited by laser ablation on (001) MgO. Journal of Materials Research, 1995, 10, 791-794.	2.6	23
159	Atomistic structure of 90Ű domain walls in ferroelectric PbTiO ₃ thin films. Philosophical Magazine A: Physics of Condensed Matter, Structure, Defects and Mechanical Properties, 1995, 71, 713-724.	0.6	143
160	Diffusion Reactions at Metal/Ceramic and Ceramic/Ceramic Interfaces. Materials Science Forum, 1994, 155-156, 331-344.	0.3	1
161	Nanostructure and chemistry of a (100)MgO/(100)GaAs interface. Applied Physics Letters, 1994, 65, 564-566.	3.3	15
162	TEM study of the structure and chemistry of a diamond/silicon interface. Journal of Materials Research, 1994, 9, 1566-1572.	2.6	27

#	Article	IF	CITATIONS
163	Quantitative high-resolution transmission electron microscopy of the incoherent Σ3 (211) boundary in Cu. Ultramicroscopy, 1994, 53, 205-221.	1.9	109
164	Thermal-stress-induced dislocations in GeSi/Si heterostructures. Journal of Crystal Growth, 1994, 137, 457-471.	1.5	22
165	Dissociation of misfit dislocation nodes in (111)GeSi/Si interfaces. Philosophical Magazine A: Physics of Condensed Matter, Structure, Defects and Mechanical Properties, 1993, 68, 1251-1272.	0.6	20
166	Dissociation of Misfit Dislocations in GeSi/{111}Si Interfaces. Materials Research Society Symposia Proceedings, 1993, 319, 165.	0.1	0
167	Theoretical prediction and direct observation of the 9Rstructure in Ag. Physical Review Letters, 1992, 69, 620-623.	7.8	157
168	Twoâ€dimensional growth of strained Ge0.85Si0.15on Si(111) by liquid phase epitaxy. Journal of Applied Physics, 1992, 72, 2083-2085.	2.5	19
169	High resolution transmission electron microscopy studies of the Ag/MgO interface. Acta Metallurgica Et Materialia, 1992, 40, S227-S236.	1.8	144
170	The influence of grain boundary inclination on the structure and energy of $if = 3$ grain boundaries in copper. Philosophical Magazine A: Physics of Condensed Matter, Structure, Defects and Mechanical Properties, 1992, 66, 991-1016.	0.6	193
171	Lattice mismatch accommodation atGeSi/{111}Si interfaces grown by liquid phase epitaxy. Physica Status Solidi A, 1992, 131, 651-662.	1.7	26
172	Liquid phase epitaxy of GeSi on {111} Si substrates: lattice defect structure and electronic properties. Journal of Crystal Growth, 1992, 118, 452-460.	1.5	13
173	HRTEM study of a Cu/Al ₂ O ₃ interface. Philosophical Magazine A: Physics of Condensed Matter, Structure, Defects and Mechanical Properties, 1991, 63, 259-277.	0.6	105
174	Germanium Concentration Profiles Across Interfaces And Close To Dislocations In Cvd Si1â^'xGex-on-Si Junctions Materials Research Society Symposia Proceedings, 1991, 238, 469.	0.1	1
175	The formation mechanism of planar defects in compound semiconductors grown epitaxially on {100} silicon substrates. Journal of Materials Research, 1989, 4, 834-842.	2.6	91
176	Hexagotnal Silicon: A New Hrem Study. Materials Research Society Symposia Proceedings, 1989, 139, 199.	0.1	2
177	On the generation of new orientations during recrystallization: Recent results on the recrystallization of tensile-deformed fcc single crystals. Progress in Materials Science, 1988, 32, 1-95.	32.8	115
178	Formation of planar defects in the epitaxial growth of GaP on Si substrate by metal organic chemicalâ€vapor deposition. Journal of Applied Physics, 1988, 64, 4526-4530.	2.5	82
179	Heteroepitaxy on (001) Silicon: Growth Mechanisms and Defect Formation Materials Research Society Symposia Proceedings, 1988, 116, 57.	0.1	45
180	High Resolution Electron Microscopy of an Alumina/Copper Interface. Materials Research Society Symposia Proceedings, 1988, 138, 557.	0.1	7

#	Article	IF	CITATIONS
181	Inversion Domain Boundary Dislocations in Heteroepitaxial Films. Materials Research Society Symposia Proceedings, 1988, 144, 189.	0.1	6
182	Recrystallization Experiments in Tensile Deformed 〈100〉- and 〈111〉-Oriented Copper Single Crysta Textures and Microstructures, 1988, 8, 383-400.	als. 0.2	2
183	High resolution electron microscopy of small precipitates. Scripta Metallurgica, 1987, 21, 1189-1194.	1.2	14
184	The decomposition kinetics of Al-1 at% Ag at 413 K studied by HREM. Physica Status Solidi A, 1987, 104, 403-416.	1.7	28
185	Ultrahigh-Strength AISI-316 Austenitic Stainless Steel Foils Through Concentrated Interstitial Carbon. SSRN Electronic Journal, 0, , .	0.4	0
186	Electronic Impact of Concentrated Interstitial Carbon on Physical Properties of AISI 316 Austenitic Stainless Steel. SSRN Electronic Journal, 0, , .	0.4	0